Use of OpenFOAM and RAMMS Avalanche to simulate the interaction of avalanches and slush flows with dams

Hafþór Örn Pétursson*, Kristín Martha Hákonardóttir and Áki Thoroddsen

Verkís, Ofanleiti 2, IS-103 Reykjavík, ICELAND
**Corresponding author, e-mail: hop (at) verkis.is*

ABSTRACT

We explore the possibilities of using two different programs to aid with the design of protection dams against snow avalanches and slushflows. The RAMMS 1.6 Avalanche module, developed by the SLF in Switzerland, was used to back-calculate large and medium sized avalanches on the Flateyri deflecting dams. We find that the program reproduces the observed avalanche run-out for the avalanches studied with an appropriate choice of avalanche volume and oblique shocks are formed in the interaction with deflecting dams. A full 3D simulation is, however, needed to study the interaction of avalanches and dams, when ballistic overflow is important for realistic results of the simulation. OpenFOAM is an open source CFD software, commonly used to simulate complex flows for engineering purposes. The software was used to simulate the interaction of a slushflow with a row of mounds and a catching dam, as a two-phase flow of Newtonian fluids, in three dimensions. The numerical solution was compared with experimental results of the interaction of water with mounds and dams. The study showed that the software may be successfully used to simulate the water–obstacle interaction and optimize the engineering design.

1. INTRODUCTION

1.1 Interaction with a deflecting dam

We use the program RAMMS Avalanche module to simulate the interaction of avalanches and deflecting dams. The frictional parameters used in the simulations have not been calibrated for large Icelandic avalanches, as was done for the program Samos (Gíslason and Jóhannesson, 2007). The software has, however, been tested for a number of large and medium-sized historical Icelandic avalanches, with the recommended frictional parameters for Swiss avalanches (Bartelt et al., 2016) with promising results. We have chosen to study in some detail two medium-sized avalanches that hit the deflecting dam at Flateyri in 1999 and 2000 and a catastrophic avalanche that hit Flateyri in 1995, see Figure 1.

The three avalanches were compared and analysed in terms of the effectiveness of the dams in a paper by Jóhannesson (2001) and the 1999 avalanche was discussed and analysed by Jóhannesson et al. (1999). An overall agreement is found in the observed run-up of the avalanches and the run-up based on back calculations of flow speed and the traditional formulation for run-up, based on energy conservation of a point mass. It is concluded that the dams will be effective for substantially larger avalanches. It is also noted that the estimated flow marks on the dams may be an overestimate of the highest run-up of the dense part of the avalanche. Both avalanches were channelized at the dam, but the avalanche upstream of the channelized part appeared unaffected by the dams. This has been interpreted in terms of the formation of an oblique shock at the dam, analogues to oblique hydraulic jumps for high Froude number free-

surface flows of water or oblique shocks for high Mach number flows of gas. An abrupt change in thickness, flow direction and density, occurs and a thicker and more dense current flows along the dam.

The oblique shock, formed at the Flateyri dam in 1999, was studied numerically by Cui et al. (2007). They found good agreement between the observed indications of an oblique shock and the simulated shock, but less so between the highest run-up marks on the dam and the maximum simulated flow depth and the observed run-out.

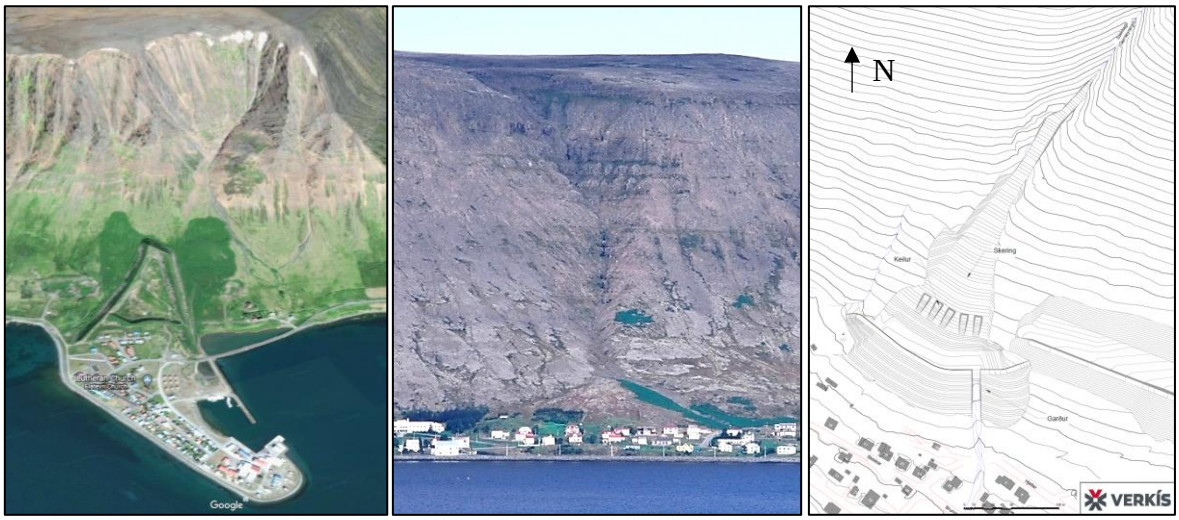

Figure 1 To the left: The Flateyri avalanche deflecting dams, built in 1996–1999 (Google Earth image, 2019). To the right: The Stekkagil ravine in Patreksfjörður, Northwestern Iceland (photo: Hákonardóttir, 2006) and the proposed design of defence structures for stopping slushflows from the gully (Verkís, draft from 2016).

1.2 **Interaction with mounds and a dam**

Previous numerical simulations of slushflows include studies of Gauer (2004) who simulated slushflows in three dimensions as a two-phase flow of a fluid and air, with the fluid as a multi-component fluid, in CFX, with and without erosion of the surrounding snow-pack and also, the much simpler approach, in RAMMS Avalanche using a single-phase, depth-averaged model, determining frictional parameters to fit observed flow speeds (Jónsson and Gauer, 2014). We choose an approach that is between the two in terms of complexity.

A full 3D simulation, using the opensource software package OpenFOAM, is used to study the interaction of a slushflow with braking mounds and a catching dam, due to the ballistic nature of the overflow. We study the proposed defence measures below the Stekkjargil ravine in Patreksfjörður, Northwestern Iceland, Figure 1. The design entails one row of 5 pc of 5.5 m high and 6 m wide, steep braking mounds and a 12 m high, steep catching dam located 70 m below the mounds. An opening in the dam, with rails, similar to debris flow defences, ensures an escape for water to the East and a spillway for water to the West. The mounds are located on the 15° slope of a debris cone. The row of mounds is located sufficiently far away from the mouth of the gully, such that debris, carried down the gully during spring and autumn flooding will not block the mounds. The distance between the mounds is 5 m, allowing vehicles to excavate debris. The design slushflow is approximately $50 \cdot 10^3$ m^3, flowing at a speed of 10 to

20 m/s, with a depth of 1 to 3 m. The design was tested in laboratory experiments described by Hákonardóttir and Ágústsdóttir (2019).

The OpenFOAM simulations allow calculations of the impact pressure at the mounds and at the dam, which is especially important for the mound design in Patreksfjörður. Pressure measurements have shown that the interaction between the dense core of a snow avalanche and an obstacle can be divided into two periods (Salm, 1964; Kotlyakov et al., 1977; Schaerer and Salway, 1980). During the first few milliseconds of the impact, a pressure peak is observed. The peak is followed by a lower base pressure with much longer duration. Pressures, on a 20 m high and 0.6 m wide pylon with a 62° wedge upstream, have been measured at the Vallée de la Sionne experimental site in Switzerland for 20 years. Sovilla et al. (2018) report pressure measurements for a slowly-moving avalanche characterized by a warm plug regime. They measure maximum pressures at the base of the pylon. The measurements do, however, not show a single pressure peak in the impact, but rather many peaks measured during the first 10 s of the flow. Jaedicke et al. (2008) measured impact pressure on an obstacle in the flow path of a slushflow, in large-scale experiments on a 30 m long chute at Weissfluhjoch, Davos, and found the highest pressures as the flow front hit the obstacles.

2. THEORY

2.1 Flateyri: Deflecting dams

The Flateyri dams were designed based on the traditional run-up equation, based on energy conservation of a point mass

$$h_u = \frac{(u \sin\gamma)^2}{2g} + h + h_s, \qquad (1)$$

where u is flow speed, γ is deflecting angle between the dam and the avalanche and g is gravitational acceleration, h is the flow depth and h_s is the thickness of the snowcover on the ground (Salm, 1990). Since 2005, dams in Iceland have been designed according to the European guidelines (Jóhannesson et al., 2009), based on the formation of an oblique shock at the dam, as has been observed in experiments with dams and granular flows (Gray et al., 2003, Hákonardóttir and Hogg, 2005). The flow depth by the dam, H may be derived from:

$$H = \frac{\tan\beta}{\tan(\beta-\gamma)} \quad \text{and} \quad \tan\gamma = \frac{4\sin\beta\cos\beta(1-Fr^2\sin^2\beta)}{-3+4\cos^2\beta(1-Fr^2\sin^2\beta)-\sqrt{1+8Fr^2\sin^2\beta}} \qquad (2)$$

where (β–γ) is the shock angle, measured from the dam axis.

The Froude number of a free-surface flow, upstream of the dam is given by

$$Fr^2 = \frac{u^2}{g\,h\cos\xi}, \qquad (3)$$

where u is flow speed, h is flow depth and ξ is the slope angle.

The European guidelines also provide a formula for the spreading of an avalanche downstream from the dam and the added flow depth due to curvature of the dam axis. Spreading is given by:

$$\varphi_{lsp} = \frac{2}{\mathrm{Fr}} - \frac{5}{3\mathrm{Fr}^3} + O\left(\frac{1}{\mathrm{Fr}^5}\right), \qquad (4)$$

which yields 11–21° for Froude numbers between 5 and 10. A value of 20° is often used for large dry-snow avalanches (Jóhannesson et al., 2009). For slower flows with Fr between 2 and

4 the formula yields 25–45°, which is consistent with observations of slower and wetter avalanches (Jóhannesson et al., 2009; Sovilla et al., 2012).

2.2 Patreksfjörður: Mounds and dam

The pressure in the initial impact of the flow with a dam or mound may be compared with pressure impact theory, derived by Cooker and Peregrine (1998). They found that the maximum value of the pressure impulse at the wall was

$$P_{max} = 0.742\rho uh, \quad (6)$$

for a rectangular wave, with the maximum located at the base of the wall. The magnitude of the dynamic pressure, that follows the pressure peak, and the avalanche exerts on an obstacle may be written as

$$P_{ref.} = c\rho u^2/2, \quad (5)$$

with the drag coefficient c and the density ρ. Schearer and Salway (1980) found c = 1, for an impact with a dam.

Jets of fluid or granular flows over relatively low obstacles, such as braking mounds, with the ratio of obstacle height to the flow depth between 1 and 5, have in laboratory experiments been observed to follow ballistic trajectories (see discussion by Hákonardóttir and Ágústsdóttir, 2019). The launch angle may be determined implicitly from an expression, derived by Yih (1979), for inviscid, irrotational flow, when the effect of gravity is negligible. The theory predicts that the deflection of the jet asymptotically approaches the angle between the upstream face of the dam and slope as the height of the dam relative to the flow depth increases.

Scaling between laboratory scale experiments, and the real situation in Patreksjförður, is discussed by Hákonardóttir and Ágústsdóttir (2019).

3. NUMERICAL APPROACH

3.1 RAMMS: Deflecting dam

The RAMMS 1.6 Avalanche module was developed by the SLF in Switzerland (Christen et al., 2010). The core of the program is a second-order numerical solution of the depth-averaged avalanche dynamics equations (identical to the shallow water equations), with a Voellmy-Salm type rheology. The following simplistic approach was chosen: Frictional parameters were chosen according to Swiss calibration recommendations (see Table 1) and the volume was chosen to fit the desired run-out. The density was kept constant at 300 kg/m^3. No entrainment was assumed. A 5x5 m grid was used, as recommended by Christen et al. (2010).

Table 1 Frictional parameters in RAMMS simulations with volume over $60 \cdot 10^3$ m^3.

	Open slope	**Channel**	**Gully**	**Flat**
Coulomb friction, μ	0.19	0.24	0.30	0.17
Velocity dependent friction, ξ (m/s^2)	2000	1500	1200	3000

3.2 **OpenFOAM: Mounds and a dam**

OpenFOAM is used to study the impact of a large slushflow down the Stekkagil ravine, with a row of braking mounds and a dam. We do not attempt to model the slushflow down the entire ravine, due to numerical complications, but rather tune the flow speed and depth at the inlet, approximately 20 m above the mounds, to the desired value. Three-dimensional multiphase simulation model, using the Volume of Fluid Method is constructed were the two-phases simulated are air and liquid. Kobayashi et al., (1994) and Jaedicki et al. (2008), concluded in their study that slush is a non-Newtonian fluid. For the sake of clear comparison with experiments and simplicity, the fluid in this study is modeled as a Newtionan fluid, with a density of 800 kg/m^3 and the viscosity of water at 0° C. OpenFOAM, however, facilitates different rheological models (OpenFOAM source code, 2018).

The simulation domain is 115 m x 32 m x 22 m (length x height x width) see Figure 2. We adopt a similar approach as in the experiments discussed by Hákonardóttir and Ágústsdóttir (2019), to study the three-dimensional nature of the fluid-mound interaction. Instead of computationally heavy, fully 3D geometry of the ravine, the cross slope is studied with two mounds, normal to the flow direction. The domain is broken into two sections (separation patch) where each section is less computationally demanding than the whole domain. Firstly, a simulation is carried out for the upper half of the domain, which includes the braking mounds. The focus is on a high resolution of the initial impact with respect to pressure at impact and the evolution of the upward propagating jet. Secondly, the two domains are merged together, and the solution of the upper half is mapped onto the lower half of the domain. The focus in the lower half is on the impact with the catching dam and the evolution of the fluid–dam impact at the upstream dam face.

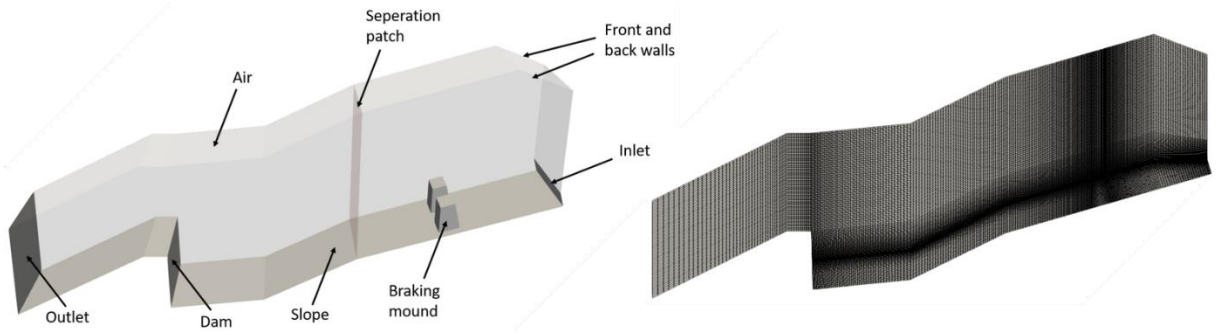

Figure 2 Left: Computational domain. Distance from the mounds to the front and back walls is 2.5 m. Right: Computational grid.

The computational grid is shown on Figure 2. The total grid size for the modelled domains are respectively for the upper domain and combined upper and lower domain: $2.51 \cdot 10^6$ and $4.35 \cdot 10^6$ cells. The grid is created using *blockMesh* meshing tool which results in a good quality mesh and facilitates adjustments to the geometry shapes.

Multiphase simulations are carried out with OpenFOAM v1812 using the *interIsoFoam* solver. The solver uses the isoadvector algorithm which captures the interface between two incompressible, isothermal, unmixable fluids (OpenFOAM source code., 2018). The method was developed by Roenby, Bredmose and Jasak (2016), where one of the main goals in their study was to improve the available VOF solver in OpenFOAM, *interFoam*. The isoadvector algorithm proved promising in preserving shapes and creating sharp interfaces between two-phases (Roenby et al., 2016). The k-ω SST model with wall functions is used for turbulence modelling.

One of the wall functions used is the *nutkRoughWallFunction*, it allows control of the roughness of the surface and is used in this project to mimic the rough terrain of the slope and resistance due to snow on the slope, using a high value for Nikuradse's sand-grain roughness, 0.25 m (OpenFOAM source code., 2018). The added roughness influences the front thickness and velocity at the tip of the slush. A slip boundary condition is applied at the the front and back walls, preventing the slush from escaping the domain but not affecting it in any other way. Second order accurate schemes are used for all divergence terms, and the first order accurate Euler scheme is used for time stepping.

4. RESULTS

4.1 Flateyri: Interaction of dry snow avalanches with deflecting dams

RAMMS simulations of the 1999 and 2000 avalanches, without and with the deflecting dams, are shown in Figure 3 and summarized in Table 2.

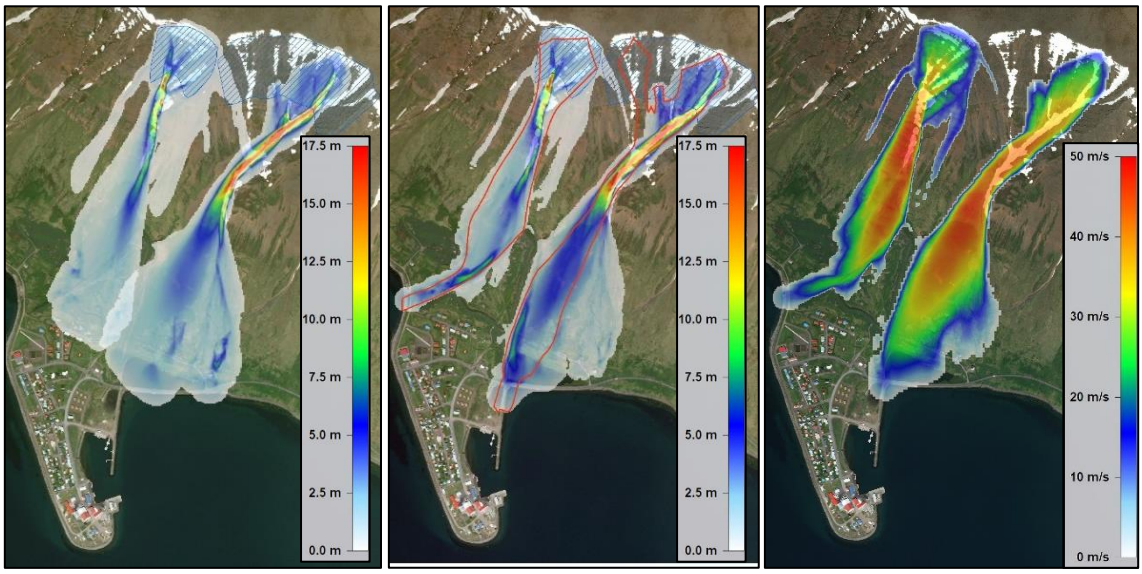

Figure 3 Maximum flow depth without and with dams (left) and maximum flow speed (right) with dams. Simulations of a dry-snow avalanche from Skollahvilft and Innra-Bæjargil Flateyri. The red lines denote the outlines of the avalanches.

Almost twice the volume in the avalanche tongue was needed to recreate the run-out of the 1999 avalanche. We conclude that a different set of frictional parameters is needed to recreate the run-out for the actual volume of snow. The curvature effects in the gully, above the dam, may also be retarding the flow too much (Fischer et al., 2012). Simulations with curvature turned off yielded higher flow speed at the dam and extended the run-out. The location of the maximum flow depth at the dam is similar between observations and simulations. The simulated flow depth at the dam is 7.5–8 m. This is comparable with the debris thickness at the dam and the thickness of the oblique shock, calculated theoretically, but not the highest flow-marks that reached 13 m. We conclude that the highest flow-marks on the dam may have been created in the initial impact and perhaps by a saltating layer on the top of the dense core of the avalanche. There is a tendency for too much lateral spreading in the simulated flow on the debris cone below the mouth of the gully as compared with the measured outline of the 1999 avalanche.

Table 2 Avalanches above Flateyri. Density in simulation ρ = 300 kg/m^3, h_s is the snow-depth on the ground

Year	Estimated volume in tongue (10^3 m^3)	Maximum run-up on dam - h_s (m)	Snow depth in release zone (m)	Volume (10^3 m^3)	Maximum run-up on dam (m)	Deflecting angle (°)	Flow depth at dam, h_1 (m)	Flow speed at dam (m/s)	Froude no.	Jump height (m), eq. (2)	Energy height + h (m), eq. (1)
	Observations			**Simulations**						**Theory**	
1995	430	-	4.5	630	17.5	23	4.0–4.5	46	7.5	19	20
1999	130	13	3.5	235	7.5–8	14	3–3.5	32	7.5	7	5
2000	110	12	1.25	90	7.5–8.5	18	2.5–3	41	7.0	12	11

The 2000 avalanche is better represented in the simulation. A similar volume was needed to recreate the observed run-out, and the highest flow marks were located at similar locations on the dam. The maximum simulated depth at the dam was 8–8.5 m. The highest flow-marks on the dam reached 12 m. The theoretically calculated maximum thickness of the oblique shock at the dam is 12 m. This flow-depth was not reached in the simulations, probably because of the narrow stream flowing towards the dam at the maximum flow speed. The simulated highest run-up on the dam is approximately 140 m farther downstream, like the flow marks on the dam suggest, and may be attributed to the curvature of the dam of approximately 700 m at that point, and centrifugal forces. No spreading to the side at the end of the dam is observed.

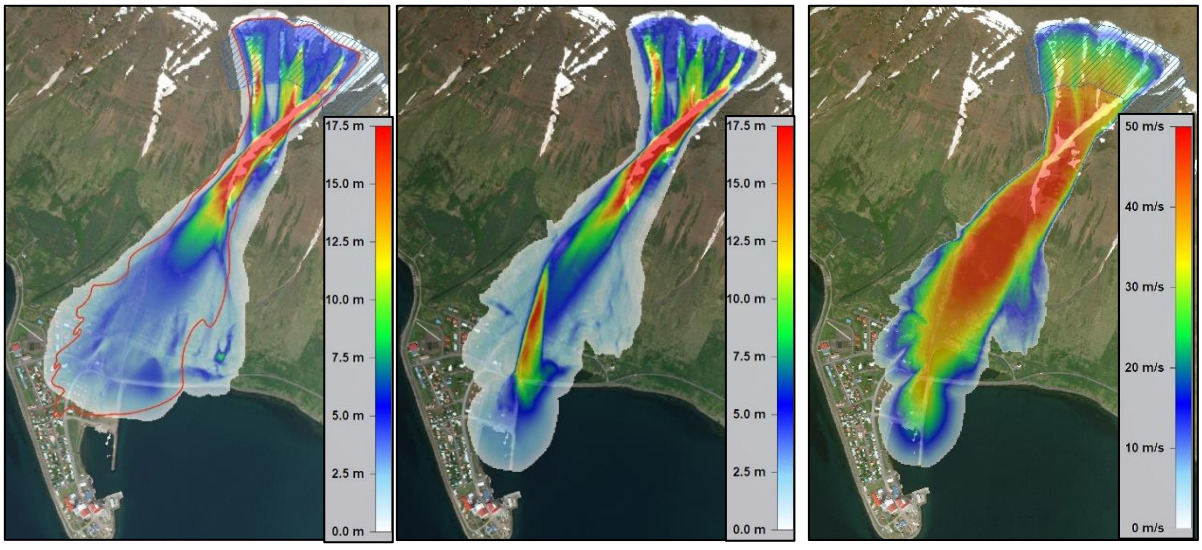

Figure 4 Maximum flow depth without and with dams (left) and maximum flow speed (right) with dams. Simulations of a dry-snow avalanche from Skollahvilft, Flateyri, with a similar run-out as the avalanche in 1995 (red line denotes the avalanche outline).

The RAMMS simulation of the 1995 avalanche is shown in Figure 4. We find that an avalanche with $630 \cdot 10^3$ m^3 is needed to reach the run-out of the avalanche, which equals 1.5 times the estimated volume in the avalanche tongue. We note more spreading to the sides, due to the

larger volume in the simulations. In the interaction of the avalanche with the now-existing deflecting dam we note that an oblique shock is formed at the dam face and the body of the avalanche is deflected to sea. The depth of the flowing stream at the dam is approximately 17.5 m, which is in agreement with back calculations of the jump depth from equations (2) and (3).

A thin part overtops the dam and at the end of the dam we find that the flow spreads at an angle of 40° from the direction of the tip of the dam, but at an angle of approximately 20° from the main dam axis. We calculate a spreading of 15°, from equation (5). We question whether the spreading may be overestimated in the simulations, due to cohesion in a denser stream flowing along the dam face. Very little spreading was observed for the 1999 avalanche that extended ca. 100 m beyond the lower end of the dam.

The flow over the dam is not correctly represented in the simulations. This part of the flow may become airborne before landing on the "wrong" side of the dam, as has been observed in experiments with granular flows (Hákonardóttir and Hogg, 2005). The simulation, however, indicates the overtopping volume that may be expected.

4.2 **Patreksfjörður: Interaction of slush with braking mounds and a catching dam**

In this chapter, the simulations of Stekkjargil ravine carried out with OpenFOAM are shown and discussed.

4.2.1 The impact with braking mounds

The flow front is 0.75 m thick, travelling at a speed of 22 m/s. The Froude number of the front is approximately 8.1. The bulk of the flow that follows has a constant flow depth of approximately 3 m, flow speed of 17 m/s and a Froude number of 3.1. The ratio of the mound height to the flow depth is approximately 2. The simulated flow may be categorized as a plug flow, with a thin shear layer, comparable to the cell size at the base, 0,25 m.

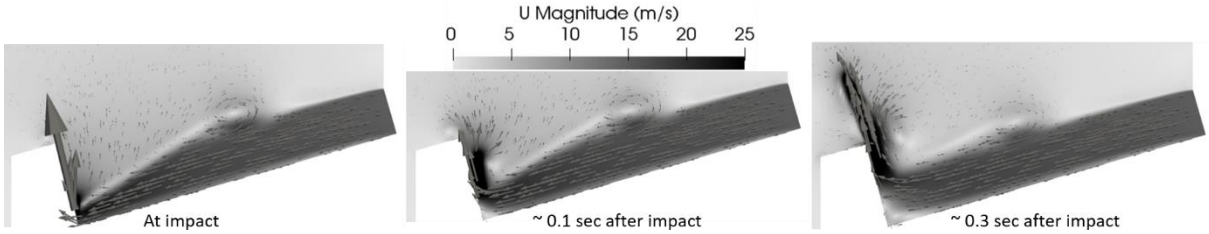

Figure 5 The upper figures show the flow speed and velocity vectors for both the fluid and the air, in the initial impact of the flow and the mounds. The boundary between the phases are clearly visible as the fluid moves towards the mounds.

A high splash is observed upon the impact with the mounds, moving upward and to the sides, see Figure 5. An enormous velocity spike is observed with a magnitude of over 6 times the inlet speed. The speed has dropped to twice the inlet speed only 0.3 s later. The splash is abrupt and rises in the direction of the mound face for 1.9 s. The splash reaches a height of 28 m, 2.9 s after impact., or 37 h_{front} and 9 h_{bulk}. The splash collapses and lands approximately 22 m upstream of the catching dam. A low velocity, circulation cell is generated at the basis of the mounds and serves as a ramp for the incoming flow and a semi-steady jet is launched over the mounds, following the initial splash and lands 15 m upstream of the catching dam, approximately 7 to 8 s after the impact with the mounds, see Figure 7. We observe identical flow behavior in the experiments presented by Hákonardóttir and Ágústsdóttir (2019), conducted at

a length scale that is approximately 10 to 20 times smaller. The Froude number in the simulations is slightly higher, but the geometry is comparable to the setup A.1.

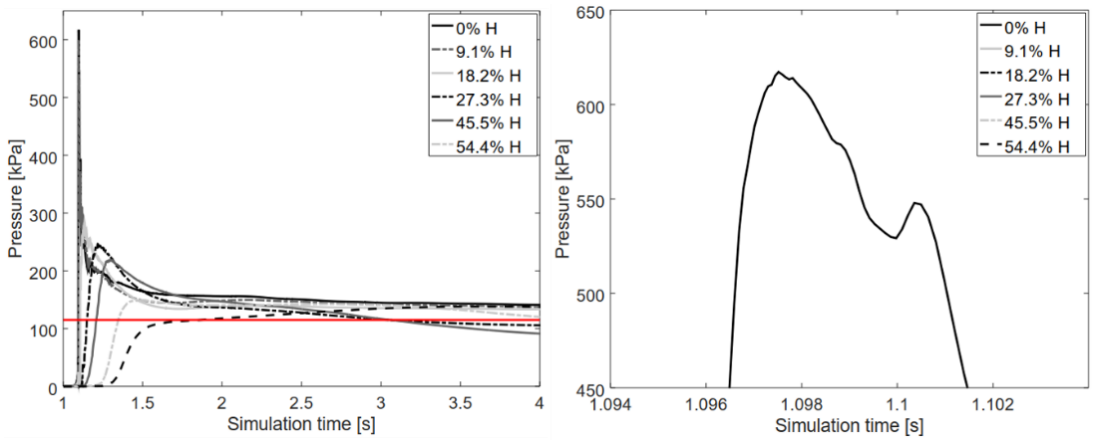

Figure 6 The pressure at the mound face as a function of time for the initial 0.4 s. The different lines show the pressure at different height at the mound face. The reference pressure for the bulk of the flow of 115 kPa is noted with a red line.

The pressure on the mounds in the impact is shown on Figure 6. The maximum pressure on the dam face is 620 kPa lasting for only approximately $5 \cdot 10^{-3}$ s. It is only the base of the mounds, lowest 0.5 m, that experience the pressure spike. The pressure spike abruptly reduces to 140 kPa and reduces further as the circulation cell enlarges. The pressure continues to reduce, due to the formation of the circulation cell, which groves with time. One may calculate the reference pressure on the mounds after the initial impact by equation (6) is 115 kPa, with $c = 1$. The maximum pressure in the initial impact may be compared with pressure impulse theory and is calculated from equation (7) to be $P_{max} = 590$ kPA, which is of the same order as in the simulations.

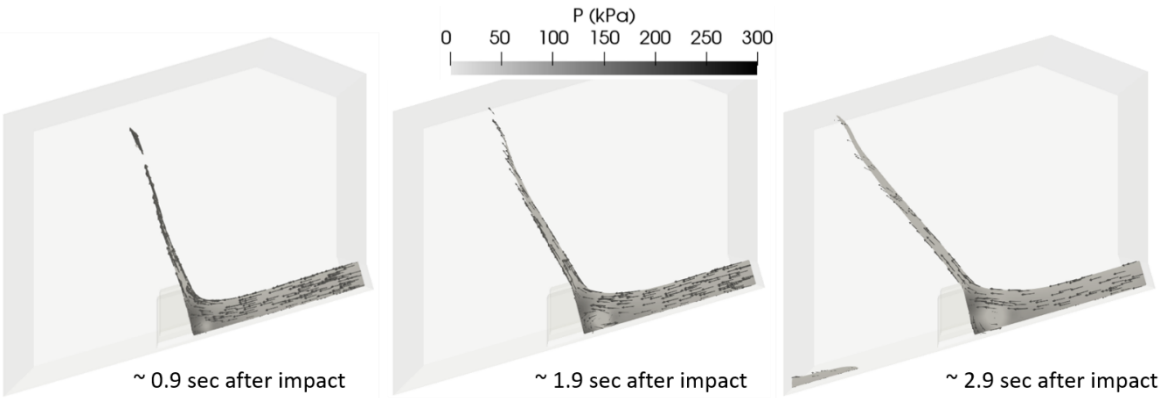

Figure 7 Time lapse figures of the impact with the mounds, 0.9, 1.9 and 2.9 s from the initial impact. The colours show the pressure and the arrows the size and the direction of the velocity vector.

The evolution of the jet over the mounds and pressure on the mound face is shown in Figure 7. A steady jet is launched over the mounds at an angle of 55° to the slope, after approximately 9 s. The angle is somewhat lower than the 65° predicted by Yih's derivation (1970) for $H/h_{bulk} = 1.8$, discussed briefly in section 2.2. The jet follows a ballistic trajectory discussed in

section 2.2. No dissipation of energy takes place at the mound face. The jet rises to a maximum height of 11–12 m, or 4 h_{bulk}, and lands approximately 45 m downstream from the mound. Drag from surrounding air does not seem to affect the trajectory of the jet.

4.2.2 The impact with the catching dam

The flow shoots between the mounds and impacts the dam, see Figure 8. A small amount of the flow spills over the dam. The part of the flow that is launched over the mounds impacts later and does not overtop the dam. A hydraulic jump, moving upwards develops after the initial impact. The flow speed downstream from the landing location of the jet is much lower than the flow speed between the mounds. It indicates that energy dissipation occurs in the landing of the jet on the slope and as the hydraulic jump moving upwards interacts with the flow shooting over the mounds.

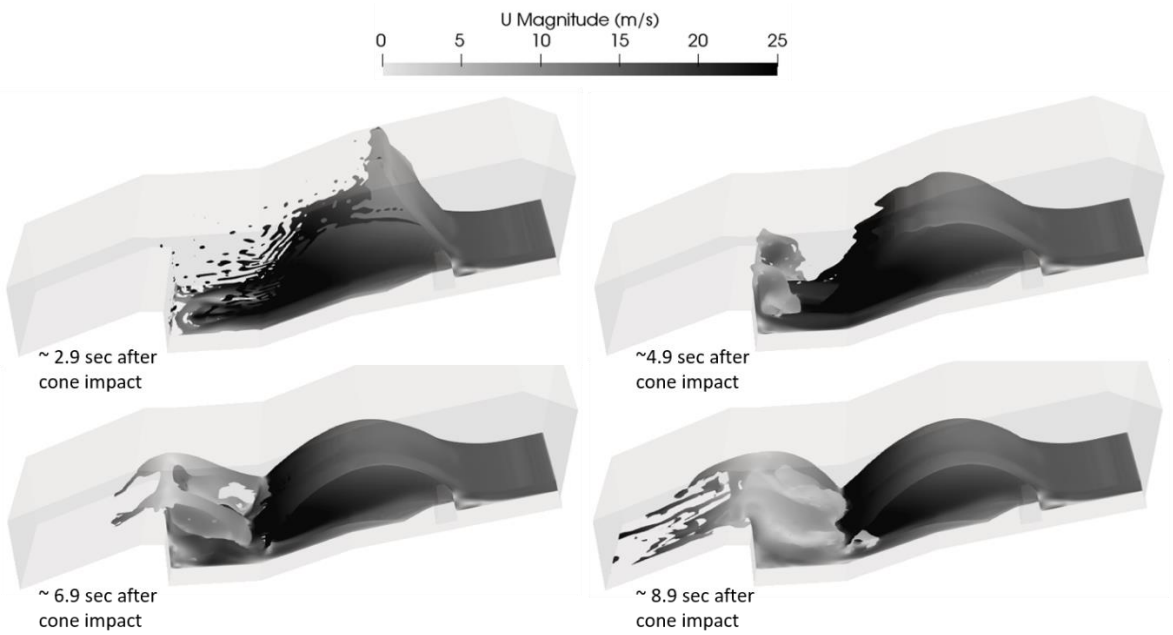

Figure 8 Time lapse figures of the flow impacting both mounds and the dam. The colours denote velocity.

CONCLUSIONS AND FURTHER STUDIES

We find that the RAMMS avalanche reproduces the observed avalanche run-out for the avalanches studied with an appropriate choice of avalanche volume. We find that 1.5 to 2 times the volume of debris in the avalanche tongue is needed to attain the desired run-out for the avalanches from Skollahvilft, while the volume of the Innra-Bæjargil avalanche was well represented by the volume in the tongue. The run-up on the dams agrees with the theory and oblique shocks are formed in the interaction with deflecting dams and the effects of dam curvature are realistic. We note that spreading downstream from the end of the dam needs to be analysed further for large avalanches with thick stream at the end of the dam. Overflow over the dam may not be correctly represented by the depth-averaged modelling.

We conclude that OpenFOAM is a valuable tool to study the interaction of fluids and obstacles and may be important in understanding the run-up onto obstacles of different shapes and the pressures exerted on the obstacles. We find that simulations in OpenFOAM reproduce the flow phenomena observed in laboratory experiments with water and mounds (Hákonardóttir and

Ágústsdóttir, 2019) and the scaling arguments presented by Hákonardóttir and Ágústsdóttir (2019) hold. We observe that energy is not dissipated at the upstream mound face, due to the formation of a circulation cell, which creates a ramp for the flow to pass smoothly over the mounds. Energy is, however, dissipated at the dam face.

Further simulations of slushflows may include studying different types of rheologies and comparing them with the Newtonian fluid used here, using a multi-component fluid for the fluid phase and ultimately being able to simulate convincingly the flow down the gully, from its release zone, with erosion of the surrounding snow-pack. For now, we will use the model for the engineering design in Patreksfjörður and look into: Different mound setups, *e.g.* with the mounds closer together, thinner and slower flows and the effects of secondary waves/releases or wave trains.

ACKNOWLEDGEMENT

The numerical calculations were financed with support of the Icelandic Avalanche and Landslide Fund and Verkís Ltd. The authors would like to thank Vigfús Arnar Jósefsson, mechanical engineer at Verkís ltd., for his contribution to the OpenFOAM simulations, Halldór Pálsson of the University of Iceland for the inspiring OpenFOAM simulations of the experiments discussed by Hákonardóttir and Ágústsdóttir (2019) and Tómas Jóhannesson of the IMO, for his review of the manuscript.

REFERENCES

Christen, M., Bartelt, P., Graf, C., McArdell, B., Gerber, W., Glover, L.D., Kowalski, J., Gruber, U., 2014. RAMMS, rapid mass movements simulation. A numerical model for snow avalanches and research and practice. *User Manual v1.6.20 Avalanche.* WSL Institue for Snow and Avalanche Research SLF. February 2014.

Christen, M., P. Bartelt, J. Kowalski., 2010a. Back calculation of the In den Arelen avalanche with RAMMS: interpretation of model results. *Ann. of Glaciol.* 51(54), 161–167.

Christen,M., Kowalski, J., Bartelt, P., 2010b. RAMMS: Numerical simulation of dense snow avalanches in three-dimensional terrain, *Cold Reg. Sci. Technol.*, 63, 1–14.

Cooker, J.M., Peregrine, D.H., 1995. Pressure-impulse theory for liquid impact problems. *J. Fluid Mech*., 297, 193–214.

Cui, X., Gray, J. M. N. T., Jóhannesson T., 2007. Deflecting dams and the formation of oblique shocks in snow avalanches at Flateyri, Iceland. *J. Geophys. Res*. 112, F04012.

Fischer, J.-T., Kowalski, J., Pudasaini, S.P., 2012. Topographic curvature effects in applied avalanche modeling. *Cold Reg. Sci. Technol.*, 74–75, 21–30.

Gíslason, E., Jóhannesson, T., 2007. *Calibration of the samosAT avalanche model for large Icelandic dry-snow avalanches*. The Icelandic Meteorological Office, report 07006.

Gray, J. M. N. T., Tai, Y. C., Noelle, S., 2003. Shock waves, dead zones and particle-free regions in rapid granular free-surface flows. *J. Fluid Mech.* 491, 161–181.

Hákonardóttir, K.M., Hogg, A.J., 2005. Oblique shocks in rapid granular flows. *Physics of Fluids*, 17, 071101, doi: 10.1063/1.1950688.

Hákonardóttir, K.M., Ágústsdóttir, K.H., 2019. The design of slushflow barriers: Laboratory experiments. In: *Proceedings to the International Symposium on Mitigative Measures against Snow Avalanches and Other Rapid Gravity Mass Flows Siglufjörður, Iceland, April 3–5.*

Jaedicke, C., Kern, M., Gauer, P., Baillifard, M.-A., Platzer, K., 2008. Chute experiments on slushflow dynamics. *Cold Reg. Sci. Technol.*, 51, 156–167.

Jóhannesson, T., 2001. Run-up of two avalanches on the deflecting dams at Flateyri, northwestern Iceland. *Ann. Glaciol.*, 32, 350–354.

Jóhannesson, T., Pétursson, O., Egilsson, J.G., Tómasson, G.G., 1999. Snjóflóðið á Flateyri 21. febrúar 1999 og áhrif varnargarða ofan byggðarinnar (The avalanche at Flateyri on February 21st, 1999 and the effectiveness of defence dams above the settlement). *Náttúrufræðingurinn*, 69(1), 3–10.

Jónsson, Á., Gauer, P., 2014. Optimizing Mitigation Measures against Slush Flows by Means of Numerical Modelling. A Case Study Longyearbyen, Svalbard. In: *Extended Abstracts of the INTERPRAVENT 2014, November 25-28, Nara, Japan*, 727–732.

Kobayashi, S., Izumi, K., Kamiishi, I., 1989. Slushflow Disasters in Japan and its Characteristics *Proceedings of the 1994 International Snow Science Workshop, Snowbird, Utah, USA*, 657-665.

Kotlyakov, V.M., Rzhevskiy, B.N., Samoylov,V.A., 1977. The dynamics of avalanching in the Khibins. *J. Glaciol*., 19, 431–439.

OpenFOAM source code. (2018) *interIsoFoam $FOAM_APP/solvers/multiphase/ interIsoFoam/InterIsoFoam.C, (v1812)*

OpenFOAM source code (2018) viscosityModel $FOAM_SRC/src/transportModels/ incompressible/viscosityModels, *(v1812)*

Roenby, J., Bredmose, H., Jasak, H., 2016 A computational method for sharp interface advection. *R. Soc. open sci. 3:160405.* http://dx.doi.org/10.1098/rsos.160405

Salm, B., 1964. Anlage zur Untersuchung dynamischer Wirkungen von bewegtem Schnee. *ZAMP*, 15, 357–375.

Salm, B., Burkard, A., Gubler, H. U., 1990. *Berechnung von Fliesslawinen. Eine Anleitung fuer Praktiker mit Bleispielen*. Davos, Eidgenössisches Institut für Schnee- und Lawinenforschung, Mitteilungen Nr. 47.

Schaerer, P.A., Salway, A.A., 1980. Seismic and impact-pressure monitoring of flowing avalanches. *J. Glaciol.*, 26, 179–187.

Sovilla, B., Sonatore, I., Bühler, Y., Margreth, S., 2012. Wet-snow avalanche interaction with a deflecting dam: field observations and numerical simulations in a case study. *Nat. Hazards Earth Syst. Sci.*, 12, 1407–1423.

Sovilla, B., Kyburz, M., Schaer, M., Margreth, S., 2018. Avalanche pressure at the Vallee de la Sionne test site: Comparison of maximum measured loads with design loads. In: *Proceedings, International Snow Science Workshop, Innsbruck, Austria, 21–25*.

Yih, C.-S., 1979. *Fluid Mechanics*, West River Press, 144–152.